CHINESE OPTICS LETTERS

Vol. 19, No. 12 | December 2021

Robust integration of nitrogen-vacancy centers in nanodiamonds to optical fiber and its application in all-optical thermometry

Ce Bian (边 策)[1], Minxuan Li (李敏轩)[1], Wei Cao (曹 蔚)[1], Manli Hu (忽满利)[1], Zhiqin Chu (褚智勤)[2*], and Ruohui Wang (王若晖)[1**]

[1] School of Physics, Northwest University, Xi'an 710127, China

[2] Department of Electrical and Electronic Engineering, Joint Appointment with School of Biomedical Sciences, The University of Hong Kong, Hong Kong, China

*Corresponding author: zqchu@eee.hku.hk

**Corresponding author: rwang@nwu.edu

Received April 9, 2021 | Accepted July 7, 2021 | Posted Online September 22, 2021

In this Letter, we developed a robust method for integrating nanodiamonds (NDs) to optical fiber. The NDs, containing nitrogen-vacancy (NV) centers, were uniformly mixed with UV adhesive before coating the end surface of a multimode fiber as a hemispherical film. The excitation and collection efficiency of NV fluorescence can be enhanced by increasing the thickness of UV adhesive film and additional aluminum film deposition. The fiber-based quantum sensor was also experimentally demonstrated for all-optical thermometry application. The variation of the refractive index of UV adhesive under different temperatures will also affect the NV collection efficiency by changing the light confinement. The demonstrated facile integration approach paves the way for developing fiber-based quantum thermometry and magnetometry.

Keywords: fiber optics sensors; fiber optics; quantum optics.

DOI: 10.3788/COL202119.120601

1. Introduction

The negatively charged nitrogen-vacancy (NV) centers in nanodiamonds (NDs) are a promising quantum sensor for various physical parameters such as magnetic field[1–4], electrical field[5,6], and temperature[7,8]. Requiring free space optical components, conventional NV-based sensing is complex and bulky[9–11]. In recent years, the method of combining optical fiber with an NV center shows great potential in simplifying the NV sensing system. In order to effectively utilize NV centers in these applications, fluorescence (FL) excitation and collection of color centers need to be enhanced. For example, Schröder *et al.*[12] reported a method by placing a pre-selected ND directly on the fiber facet. The photon collection efficiency is equivalent to a far-field collection via an objective with a numerical aperture of 0.82. However, the positioning of a single ND particle is complicated, and precise instruments such as an atomic force microscope (AFM) are needed. Fedotov *et al.*[13] proposed a guidance mode coupling mechanism for ND using hollow core photonic crystal fibers. The embedding process of ND particles in an optical fiber needs precise alignment, which is relatively complex. Liu *et al.*[14] proposed an integration method depositing NDs on a tapered fiber, and an effective coupling has been achieved. The constructed system features excellent portability, convenient fabrication, and potential for further integration. Nevertheless, tapered optical fibers cannot meet the structural requirements of probes in complex environments. Besides NDs, the microdiamond has been also integrated on the optical fiber for temperature measurement. A microdiamond contains more NV centers than an ND, but the NV centers in a microdiamond have poor optical and spin properties. The FL in NDs will easily leak out, which enables us to further improve the collection efficiency[15].

In this Letter, a facile integration method for an ND with a large number of NV centers has been developed. Specifically, NDs were mixed with UV adhesive in a proper ratio and then coated onto the fiber end surface. The UV adhesive had a very high adhesion to quartz material after curing[16,17], which guaranteed a robust conjugation of NDs to fiber end surface. Compared with the temperature sensing based on the optically detected magnetic resonance technique[8,18], the current configuration facilitating all-optical thermometry has the advantages of being simple, straightforward[7], and readily implementable in any spectrometer. We demonstrated that

the excitation/collection efficiency was directly related to the thickness of the coated NDs film on the fiber end surface. This fiber-based NV sensor has a particularly promising prospect in real applications owing to its good portability, manufacturing, stability, and low cost.

2. Fabrication of Probe

The available NDs are produced by the high pressure and high temperature (HPHT) method, and the negatively charged NV centers are formed upon annealing of the irradiated nanocrystallites at 800°C for 2 h. On average, the N concentration is on the order of 100 ppm (parts per million), and the number of NVs is ~1000 per particle. The NDs in the adhesive were prepared by first mixing 0.1 mg diamond powder of 100 nm diameter and 5 μL optical adhesive (Norland optical adhesive 68, $n = 1.58$). The mixed solution was then dispersed for 30 min using ultrasound to form a uniform material with a concentration of 20 mg/mL prior to film deposition. Second, the uniform material was coated on a multimode fiber's (MMF) end surface (GI2017-A, YOFC, core diameter: 105 μm, cladding diameter: 125 μm, NA: 0.30 ± 0.02).

As shown in Fig. 1(a), the manufacturing process of the probe is mainly divided into three steps. Step 1 is to dip the ND mixed UV adhesive on the end face of MMF2 (medium of optical fiber). Step 2 is to aim MMF1 (probe) at MMF2 and make the two end faces contact slowly. In step 3, MMF2 is moved in the opposite direction, and part of the UV adhesive remains on the end face of MMF1 due to adsorption, by controlling the contact area between the UV adhesive and the MMF1 end face, where hemispherical films of different thicknesses can be obtained.

All of the above operations were carried out on a 3D displacement platform under a microscope. The film was finally cured after half an hour with a UV lamp, and the NDs were firmly fixed

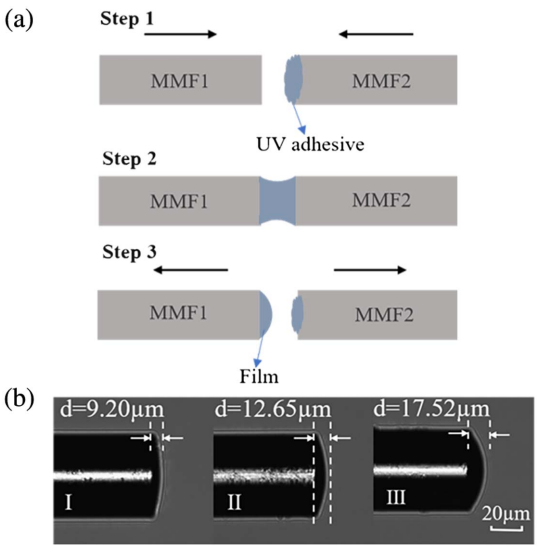

Fig. 1. (a) Fabrication steps of the sensing probe; (b) microscopic images of the sensor probes with different thickness film.

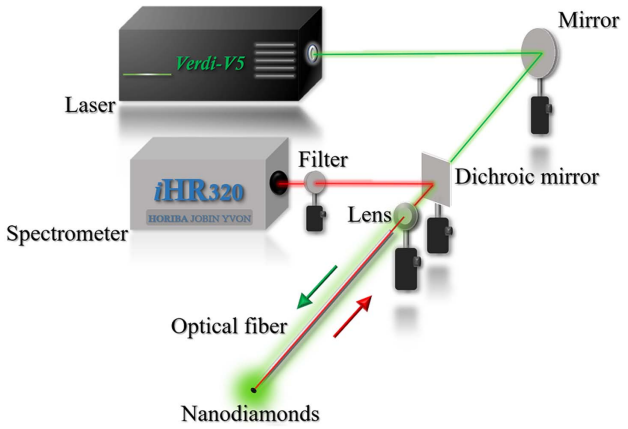

Fig. 2. Schematic diagram of the experimental setup.

in the optical fiber end surface. Figure 1(b) shows three sensing probes with thickness (d) of (I) 9.20 μm, (II) 12.65 μm, and (III) 17.52 μm, respectively. The volume ratio of NDs in the film is only 1:175, and the NDs only account for a relatively small part. The number of NDs in the film can be easily tuned by changing the ratio of the NDs in the UV adhesive.

Figure 2 schematically depicts the experimental setup for optical measurement. A 532 nm laser was focused on the coated NDs on the end face of the MMF through a dichromatic mirror and lens, and the generated FL signal was then directed to the spectrometer through the original channel. A long pass filter (600 nm) was placed in front of the spectrometer (exposure time: 0.1 s) to filter out the pump laser.

3. Results and Discussion

In order to enhance the excitation and collection efficiency of FL signals, we coated an aluminum film with a thickness of 30–50 nm on the surface of the NDs film using the magnetron sputtering method. Figures 3(a)–3(c) show the microscopic images of the cross-section view of the uncoated fiber facet with only UV adhesive and aluminum film on the UV adhesive, respectively. As shown in Fig. 3(a), we can clearly see that the light reflected on the optical fiber facet is very uniform and bright when no material is coated, and, in Fig. 3(b), we can see the rough texture of the surface after curing of the UV adhesive. The spot in the center of the film was irregular because the reflected light was scattered by the rough surface. The brighter light spot in the center, as shown in Fig. 3(c), indicated the effective coating of the aluminum film as a reflective layer, which could also be seen by the SEM image shown in Fig. 3(d).

We compared the FL energy of the probe before and after coating in water. As shown in Fig. 4 under different excitation laser power, the FL energy collected by the aluminum film increased by 12.0%, 16.3%, and 22.4%, respectively. The FL signal enhancement might be caused by the following two reasons. First, the green light was reflected by the aluminum film, improving the excitation efficiency. Second, part of the excited

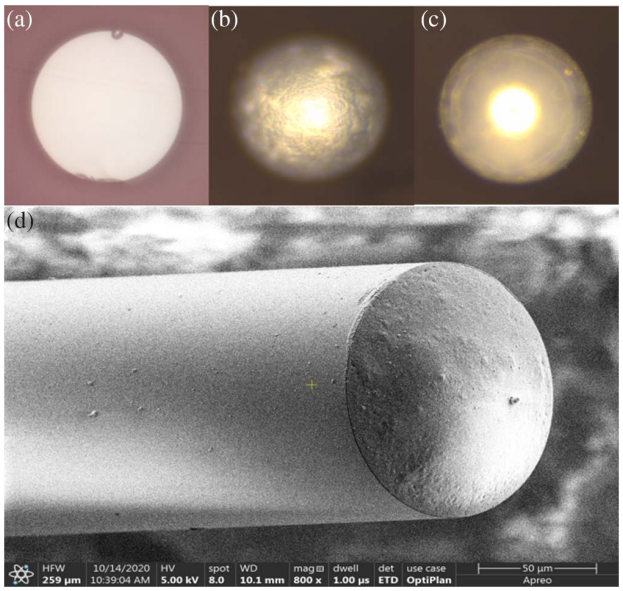

Fig. 3. Microscopic images of the cross-section view of (a) uncoated fiber facet, (b) facet only coated with UV adhesive, and (c) facet with aluminum film coated on UV adhesive; (d) SEM image of the probe after aluminum film coating.

FL is reflected by the aluminum film and then re-coupled into the optical fiber, further improving the collection efficiency. We believe that the collection efficiency can be further enhanced by optimizing the coating quality.

The impact of film thickness on the FL collection efficiency was investigated by simulation and experiment. The simulated results of FL collection using geometrical optics method are shown in Fig. 5. In the numerical investigation, we considered that the FL signal excited by NDs containing an NV center would be reflected back to the optical fiber after interacting with the aluminum film. The refractive indices of the diamond, optical fiber core, and cladding are set to be 2.4, 1.45, and 1.44, respectively. For the simulated FL collection shown in Fig. 5,

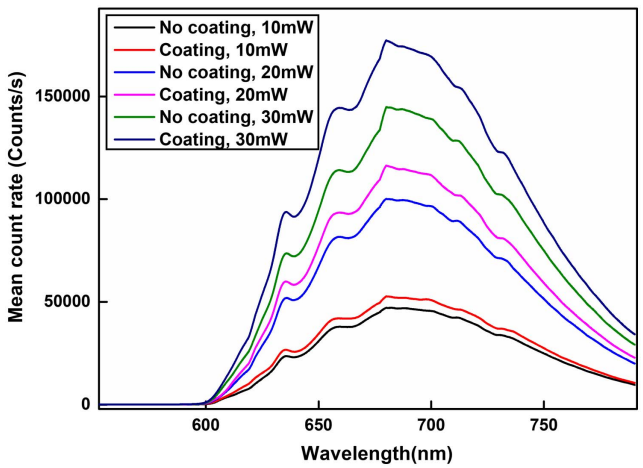

Fig. 4. FL energy of probe I before and after coating with aluminum under the different excitation laser powers.

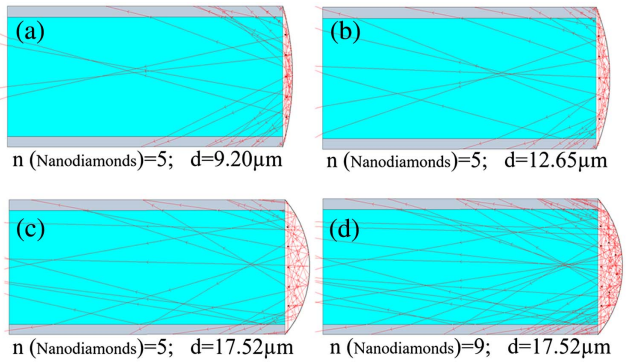

Fig. 5. Ray tracing simulations are shown in (a)–(d). The simulations are conducted using *Optgeo*.

we assumed five NDs evenly distributed in the UV adhesive. By changing the thickness of the film, it can be seen that the FL signal collected by the optical fiber core increases with the decrease of the radius of the hemispherical NDs coating. With the decrease of the radius of curvature, the convergence effect of aluminum film becomes more and more obvious, and therefore more FL signals are reflected back into the optical fiber core. Besides the curvature of the NDs coating, the number of the NDs also affects the FL signal enhancement with the variation of the film thickness. For example, the radius of curvature is the same as that of the Fig. 5(c), while the number of positioned NDs was increased to nine [Fig. 5(d)]. The simulated results showed that the increased number of NDs would enhance the FL signal collection. In experiment, we set the laser power to 20 mW and verified the FL collection of the three sensing probes in water. In Fig. 6, it can be seen that the probes with the 9.20 μm, 12.65 μm, and 17.52 μm UV adhesive film coating correspond to the collected FL energy of 11,745 counts, 20,287 counts, and 42,549 counts, respectively. With the increase of UV adhesive thickness, the FL signal energy is significantly enhanced, which is consistent with the simulation results.

Finally, the fabricated fiber-based quantum probe was demonstrated for temperature sensing with an input laser power

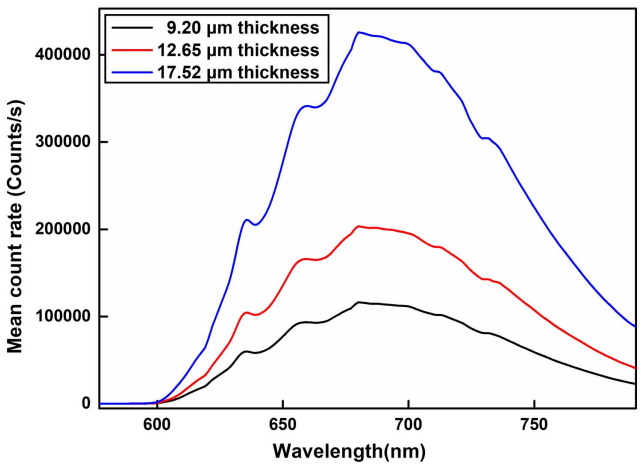

Fig. 6. Collected FL energy of three probes with different thickness.

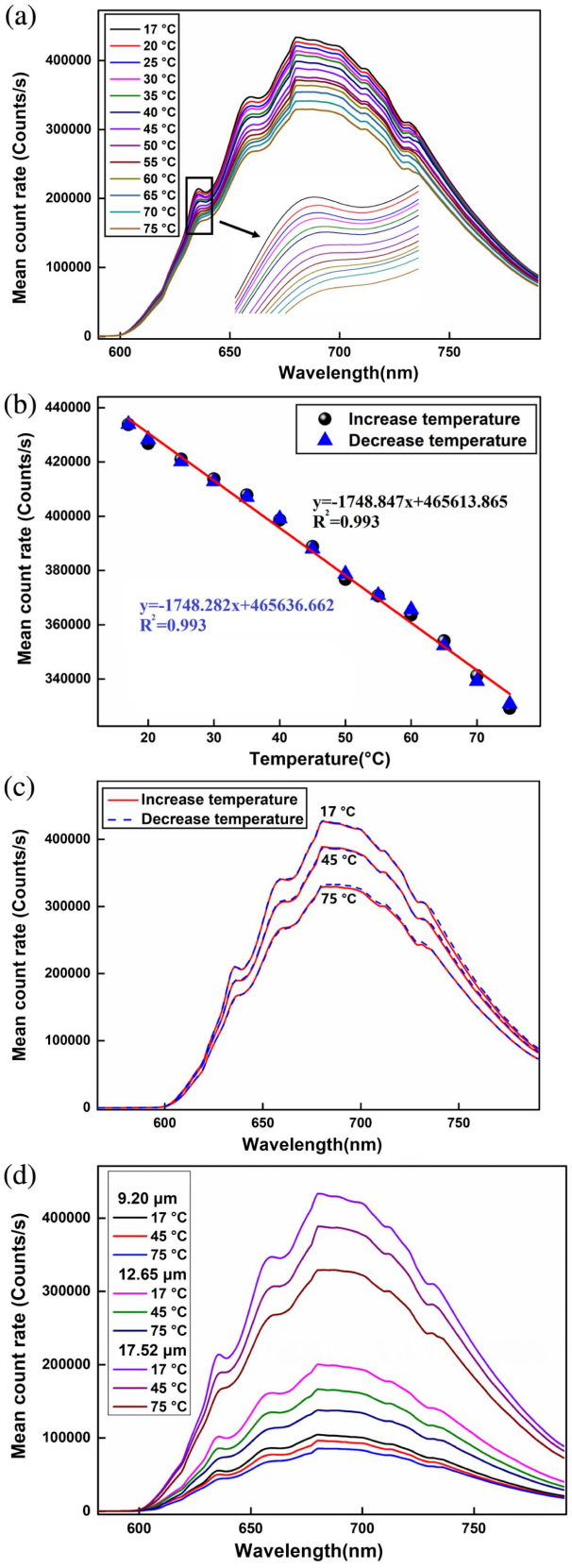

Fig. 7. (a) Temperature dependent FL signal spectra of probe III; (b) temperature increase and decrease calibration curve of probe III; (c) comparison of temperature increase and decrease of probe III; (d) trend of FL energy attenuation of the three sensors compared at 17°C, 45°C, and 75°C.

of 20 mW. The three sensors were placed into a water bath, and the FL signals at the initial temperature of 17°C were recorded. The FL spectra were recorded at intervals of 5°C from 20°C to 75°C. Figure 7(a) shows the temperature response spectral lines of probe III. It can be seen that the zero-phonon line (ZPL) has a significant broadening effect and shifts with temperature variation. The temperature response is 0.034 nm/°C, and it is consistent with the experimental phenomenon in Refs. [7,19]. Nonetheless, it is not enough to obtain the temperature sensitivity of the sensor only by reading the drift information of ZPL, because the too little sensitivity cannot meet the temperature measurement requirements in some specific environments.

However, we found that as the temperature increased the energy of the main excitation peak, ZPL also decreased. This was attributed to the fact that the thermal expansion induced refractive index decrease of the UV adhesive film caused the leakage of excitation light and FL signals. The FL decreasing due to an increase of non-radiative pathways in the high temperature also contributed to the energy decrease of ZPL[20]. However, according to the results shown in Ref. [7], we can judge that the thermal expansion of UV adhesive is still the main reason for the decrease of FL energy[7]. As shown in Fig. 7(b), we plot the FL intensity as a function of temperature, including temperature increase and decrease. It can be seen that at the same temperature the FL intensity obtained in the process of increasing and decreasing temperature is almost the same, and the slope difference between the two fitting curves is only 0.565. Figure 7(c) shows the spectra of increasing and decreasing the temperature, and the good coincidence proves the probe's high reproducibility. In Fig. 7(d), the trend of FL energy attenuation can be intuitively seen by comparing the FL spectra of the three sensors at 17°C, 45°C, and 75°C. The thicker the UV adhesive, the more obvious the thermal expansion effect. We calculated the ratio of the energy attenuation of these three probes with the increase of temperature. When the film thickness is 9.20 μm, 12.65 μm, and 17.52 μm, respectively, for every 1°C increase in temperature, the corresponding energy decreases by 32,296 counts, 106,195 counts, and 174,840 counts. According to the method in Refs. [21,22], the sensitivity of probe III was calculated to be 1.97 $kHz^{-1/2}$[21,22].

4. Conclusion

In summary, a simple integration method for NDs to fiber has been proposed. The simulated and experimental results showed that the excitation and collection efficiency of the FL signal can be enhanced by increasing the thickness of NDs adhesive coating. In addition, coating the NDs adhesive surface with a metal film will further increase the FL signal of the sensor. In the temperature measurement, for every 1°C increase, the energy of FL of the sensing probe decreases by 174,840 counts. The proposed NDs integration approach paves the way for developing fiber-based NV thermometry and magnetometry.

Acknowledgement

This work was supported by the National Natural Science Foundation of China (No. 62075181), Z. Chu acknowledges financial support from the HKU Start-Up Grant and the Seed Fund (No. 202011159019).

References

1. V. Fedotov, S. M. Blakley, E. E. Serebryannikov, P. Hemmer, M. O. Scully, and A. M. Zheltikov, "High-resolution magnetic field imaging with a nitrogen-vacancy diamond sensor integrated with a photonic-crystal fiber," Opt. Lett. **41**, 472 (2016).
2. S. M. Blakley, I. V. Fedotov, S. Y. Kilin, and A. M. Zheltikov, "Room-temperature magnetic gradiometry with fiber-coupled nitrogen-vacancy centers in diamond," Opt. Lett. **40**, 3727 (2015).
3. A. M. Wojciechowski, P. Nakonieczna, M. Mrózek, K. Sycz, A. Kruk, M. Ficek, M. Głowacki, R. Bogdanowicz, and W. Gawlik, "Optical magnetometry based on nanodiamonds with nitrogen-vacancy color centers," Materials **12**, 2951 (2019).
4. B. W. Zhao, Y. Dong, S. C. Zhang, X. D. Chen, W. Zhu, and F. W. Sun, "Improving the NV generation efficiency by electron irradiation," Chin. Opt. Lett. **18**, 080201 (2020).
5. F. Dolde, H. Fedder, M. W. Doherty, T. Nöbauer, F. Rempp, G. Balasubramanian, T. Wolf, F. Reinhard, L. C. L. Hollenberg, F. Jelezko, and J. Wrachtrup, "Electric-field sensing using single diamond spins," Nat. Phys. **7**, 459 (2011).
6. F. Dolde, M. W. Doherty, J. Michl, T. Nöbauer, F. Rempp, G. Balasubramanian, F. Jakobi, N. B. Manson, and J. Wrachtrup, "Nanoscale detection of a single fundamental charge in ambient conditions using the NV-center in diamond," Phys. Rev. Lett. **112**, 097603 (2014).
7. P. C. Tsai, C. P. Epperla, J. S. Huang, O. Y. Chen, C. C. Wu, and H. C. Chang, "Measuring nanoscale thermostability of cell membranes with single gold–diamond nanohybrids," Angewandte **56**, 3025 (2017).
8. I. V. Fedotov, S. M. Blakley, E. E. Serebryannikov, N. A. Safronov, V. L. Velichansky, M. O. Scully, and A. M. Zheltikov, "Fiber-based thermometry using optically detected magnetic resonance," Appl. Phys. Lett. **105**, 261109 (2014).
9. S. Bogdanović, S. B. van Dam, C. Bonato, L. C. Coenen, A. J. Zwerver, B. Hensen, M. S. Z. Liddy, T. Fink, A. Reiserer, M. Lončar, and R. Hanson, "Design and low-temperature characterization of a tunable microcavity for diamond-based quantum networks," Appl. Phys. Lett. **110**, 171103 (2017).
10. M. Gregor, R. Henze, T. Schröder, and O. Benson, "On-demand positioning of a preselected quantum emitter on a fiber-coupled toroidal microresonator," Appl. Phys. Lett. **95**, 153110 (2009).
11. S. Bogdanović, M. S. Z. Liddy, S. B. van Dam, L. C. Coenen, T. Fink, M. Lončar, and R. Hanson, "Robust nano-fabrication of an integrated platform for spin control in a tunable microcavity," APL Photon. **2**, 126101 (2017).
12. T. Schröder, A. W. Schell, G. Kewes, T. Aichele, and O. Benson, "Fiber-integrated diamond-based single photon source," Nano. Lett. **11**, 198 (2011).
13. I. V. Fedotov, N. A. Safronov, Y. A. Shandarov, A. A. Lanin, A. B. Fedotov, S. Y. Kilin, K. Sakoda, M. O. Scully, and A. M. Zheltikov, "Guided-wave-coupled nitrogen vacancies in nanodiamond doped photonic-crystal fibers," Appl. Phys. Lett. **101**, 031106 (2012).
14. X. D. Liu, J. M. Cui, F. W. Sun, X. R. Song, F. P. Feng, J. F. Wang, W. Zhu, L. R. Lou, and G. Z. Wang, "Fiber-integrated diamond-based magnetometer," Appl. Phys. Lett. **103**, 143105 (2013).
15. S. M. Blakley, C. Vincent, I. V. Fedotov, X. H. Liu, K. Sower, D. Nodurft, J. Liu, X. H. Liu, V. N. Agafonov, V. A. Davydov, A. V. Akimov, and A. M. Zheltikov, "Photonic-crystal-fiber quantum probes for high-resolution thermal imaging," Phys. Rev. Appl. **13**, 044048 (2020).
16. P. A. Mohammed, "Optical and mechanical properties of self-written polymer waveguide between single mode optical fibers using UV photocurable monomer system," Eur. Polym. J. **139**, 109950 (2020).
17. K. L. Li, J. B. Du, W. H. Shen, J. C. Liu, and Z. Y. He, "Improved optical coupling based on a concave cavity lens fabricated by optical fiber facet etching," Chin. Opt. Lett. **19**, 050602 (2021).
18. J. P. Tetienne, A. Lombard, D. A. Simpson, C. Ritchie, J. Lu, P. Mulvaney, and L. C. L. Hollenberg, "Scanning nanospin ensemble microscope for nanoscale magnetic and thermal imaging," Nano. Lett. **16**, 326 (2016).
19. B. Dong, C. K. Shi, Z. W. Xu, K. Y. Wang, H. H. Luo, F. W. Sun, P. F. Wang, E. Wu, K. Zhang, J. Y. Liu, Y. Song, and Y. X. Fan, "Temperature dependence of optical centers in Ib diamond characterized by photoluminescence spectra," Diamond Relat. Mater. **116**, 108389 (2021).
20. D. W. Duan, V. K. Kavatamane, S. R. Arumugam, G. Rahane, G. X. Du, Y. K. Tzeng, H. C. Chang, and G. Balasubramanian, "Laser-induced heating in a high-density ensemble of nitrogen-vacancy centers in diamond and its effects on quantum sensing," Opt. Lett. **44**, 2851 (2019).
21. T. Plakhotnik, M. W. Doherty, J. H. Cole, R. Chapman, and N. B. Manson, "All-optical thermometry and thermal properties of the optically detected spin resonances of the NV-center in nanodiamond," Nano. Lett. **14**, 4989 (2014).
22. P. R. Bargo, S. A. Prahl, and S. L. Jacques, "Collection efficiency of a single optical fiber in turbid media for reflectance spectroscopy," Appl. Opt. **42**, 3187 (2003).